



Heme Oxygenase Inhibition Sensitizes Neuroblastoma Cells to Carfilzomib

Ignazio Barbagallo¹ · Cesarina Giallongo²  · Giovanni Li Volti² · Alfio Distefano² · Giuseppina Camiolo² · Marco Raffaele¹ · Loredana Salerno¹ · Valeria Pittalà¹ · Valeria Sorrenti¹ · Roberto Avola² · Michelino Di Rosa² · Luca Vanella¹ · Francesco Di Raimondo³ · Daniele Tibullo²

Received: 16 March 2018 / Accepted: 15 May 2018 / Published online: 10 June 2018
© Springer Science+Business Media, LLC, part of Springer Nature 2018

Abstract

Neuroblastoma (NB) is an embryonic malignancy affecting the physiological development of adrenal medulla and paravertebral sympathetic ganglia in early infancy. Proteasome inhibitors (PIs) (i.e., carfilzomib (CFZ)) may represent a possible pharmacological treatment for solid tumors including NB. In the present study, we tested the effect of a novel non-competitive inhibitor of heme oxygenase-1 (HO-1), LS1/71, as a possible adjuvant therapy for the efficacy of CFZ in neuroblastoma cells. Our results showed that CFZ increased both HO-1 gene expression (about 18-fold) and HO activity (about 8-fold), following activation of the ER stress pathway. The involvement of HO-1 in CFZ-mediated cytotoxicity was further confirmed by the protective effect of pharmacological induction of HO-1, significantly attenuating cytotoxicity. In addition, HO-1 selective inhibition by a specific siRNA increased the cytotoxic effect following CFZ treatment in NB whereas SnMP, a competitive pharmacological inhibitor of HO, showed no changes in cytotoxicity. Our data suggest that treatment with CFZ produces ER stress in NB without activation of CHOP-mediated apoptosis, whereas co-treatment with CFZ and LS1/71 led to apoptosis activation and CHOP expression induction. In conclusion, our study showed that treatment with the non-competitive inhibitor of HO-1, LS1 / 71, increased cytotoxicity mediated by CFZ, triggering apoptosis following ER stress activation. These results suggest that PIs may represent a possible pharmacological treatment for solid tumors and that HO-1 inhibition may represent a possible strategy to overcome chemoresistance and increase the efficacy of chemotherapeutic regimens.

Keywords Heme oxygenase · Inhibitors · Proteasome · Neuroblastoma · Carfilzomib

Introduction

Neuroblastoma (NB) is an embryonal malignancy that affects normal development of the adrenal medulla and paravertebral sympathetic ganglia in early childhood [1]. The main drivers of NB formation are neural crest cell-derived sympathoadrenal cells that undergo abnormal genetic arrangements. In order to maintaining their proliferative

potential such cells regulate intracellular protein content homeostasis through the ubiquitin proteasome system. Therefore, cancer cells usually have higher proteasome activity and are more sensitive to inhibition of the proteasome when compared to normal cells. Proteasome inhibition leads to the accumulation of misfolded proteins, which results in endoplasmic reticulum (ER) stress, unfolded protein response (UPR), and apoptosis and thus representing a possible molecular target for pharmacological strategies [2, 3]. Currently, reversible and irreversible inhibitors (PIs) of the 26S proteasome are used for multiple myeloma (MM) treatment. In addition, previous studies showed that proteasome could be a therapeutic target in NB, and therefore, proteasome inhibition may represent a potential therapeutic strategy for treating NB patients [4–6]. To this regard, previous studies showed the efficacy of bortezomib treatment, a reversible PI, on neuroblastoma [7, 8]. Similarly, another recent study indicated that carfilzomib (CFZ), an irreversible PI, induces apoptosis and sensitizes NB cells to

✉ Cesarina Giallongo
cesarinagiallongo@yahoo.it

¹ Department of Drug Science, Biochemistry Section, University of Catania, Viale A. Doria 6, 95125 Catania, Italy

² Department of Biomedical and Biotechnological Sciences, University of Catania, Via S. Sofia, 97, 95125 Catania, Italy

³ Department of Surgery, Medical and Surgical Specialties, University of Catania, Via Santa Sofia, 78, 95123 Catania, Italy

doxorubicin-induced apoptosis [5]. However, the efficacy of PIs could be limited by the induction of the antioxidant Nrf2-dependent cell response, in tumor cells after chemotherapy [9–12]. To this regard, bortezomib treatment was found to decrease the expression of Keap-1, the cytosolic inhibitor of Nrf2 increasing its translocation into the nucleus. Among various Nrf2-targeted genes, heme oxygenase 1 (HO-1) has been shown to play a major role in drug resistance and regulation of cancer cell redox homeostasis [13, 14]. HO, exists in two different isoforms, HO-1 (inducible isoform) and HO-2 (constitutive isoform), catalyzing the rate-limiting step in heme degradation, resulting in the formation of carbon monoxide (CO), iron and biliverdin. HO-1 is considered a master regulator of antioxidant response and recent experimental evidence has shown its involvement in cancer cell biology protecting cancer cells, improving their survival and their resistance to anticancer treatment [13, 15–18]. Increased HO-1 expression has been observed in various human tumors both under basal conditions and following different anticancer treatments and thus suggesting that HO-1 and its by-products may have an important role in the development of a resistant phenotype [19–24]. To this regard, Furfaro et al. showed that in HTLA-230 NB cells HO-1 upregulation drives the resistance to proteasome inhibition. Furthermore, the authors also showed that the inhibition of HO activity, significantly improved the proapoptotic effect of PI and resulting in a significant reduction of the dose of PI [7].

However, the major bias of previous published manuscripts dealing with HO activity inhibition is the use of compounds inhibiting the activity of both HO isoforms (i.e., SnMP), other heme-containing enzymes, and therefore, it is not possible to clearly enucleate the effects connected to HO-1 enzymatic activity from the protein expression itself [25]. To solve this issue, our research interest was focused on the optimization of a new class ofazole-based non-competitive HO-1 inhibitors [26–29].

The present work was directed at evaluating the role of HO-1 specific activity in neuroblastoma cells following treatment with LS1/71, a non-competitive specific inhibitor of HO-1 activity and how it may impact on CFZ mediated cytotoxicity.

Materials and Methods

Cell Cultures and Treatments

NB cells SH-SY5Y were cultured in DMEM supplemented with 10% FBS and 1% penicillin/streptomycin at 37 °C and 5% CO₂. CFZ was added for 24 h alone and in combination with LS1/71 (imidazole derivate)

(synthesized as previous described [30, 31]), SnMP (10 μM), and hemin at different concentrations (2, 10, and 50 μM). All agents were diluted directly in cell culture medium. NB cells were also transfected by short interfering (si)RNAs. In particular, *HMOX-1* siRNA and control siRNA was synthesized by Guangzhou RiboBio Co., Ltd. (Guangzhou, China). The sequence of *HMOX-1* siRNA was as follows: sense, 5'-CCA GCA ACA AAG UGC AAG AdTdT-3', and antisense, 3'-dTdTGGUCGUUGUUUCACGUUCU-5. NB cell lines were transfected with 50 nM siRNA using RNAiMAX transfection reagent (Invitrogen Life Technologies, Carlsbad, CA, USA) according to the manufacturer's instructions.

Cell Viability Assay

Cell viability was assessed using ATPlite 1step assay (PerkinElmer, Milan, Italy) according to the manufacturers' protocol. Briefly, the 96-well black culture plate was taken from the incubator and equilibrated at room temperature for 30 min. Subsequently, to each well containing 100 μl of the cell suspension (5×10^5 cells/ml), 100 μl of reconstituted reagent was added and the plate was shaken for 20 min at 700 rpm using orbital shaker (Stuart Scientific, Staffordshire, UK). The luminescence was measured using Victor3 (PerkinElmer, Milan, Italy). Viability of the cells was expressed as percentage of vitality of untreated cells.

Measurement of HO Enzymatic Activity

Total HO activity was determined in cell lysate by measuring the bilirubin formation using the difference in absorbance at 464 to 530 nm as described by Ryter et al. [32].

Reaction mixtures (500 μL) consisted of 20 mM Tris-HCl, pH 7.4, (1 mg/mL, Thermo Fisher Scientific, Italy) cell lysate, 0.5–2 mg/mL biliverdin reductase, 1 mM NADPH, 2 mM glucose 6-phosphate (G6P), 1 U G6P dehydrogenase (Sigma-Aldrich, Italy), 25 μM hemin, 10 μL of DMSO (Sigma-Aldrich, Italy) (or the same volume of DMSO solution of imatinib or compound 5i or 5j to a final concentration of 10 μM). Incubations were carried out for 60 min at 37 °C in a circulating water bath in the dark. Reactions were stopped by adding 1 volume of chloroform. After recovering the chloroform phase, the amount of bilirubin formed was measured with a double-beam spectrophotometer as OD_{464–530} nm (extinction coefficient, 40 mM/cm for bilirubin). One unit of the enzyme was defined as the amount of enzyme catalyzing the formation of 1 nmol of bilirubin/mg protein/h.

Gene Expression Analysis by Real-Time PCR (qRT-PCR)

RNA was extracted by TRIzol reagent (Invitrogen, Carlsbad, CA, USA). First-strand cDNA was then synthesized with Applied Biosystem (Foster City, CA, USA) reverse transcription reagent. HO-1 mRNA expression was assessed by TaqMan Gene Expression, Applied Biosystem and quantified using a fluorescence-based real-time detection method by 7900HT Fast Real Time PCR System (Life technologies, Carlsbad, CA, USA). For each sample, the relative expression level of HO-1 (Hs01110250_m1), CHOP (Hs00358796_g1), BAX (Hs00180269_m1), BFAF (bifunctional apoptosis regulator, Hs01062109_m1), Irel alpha (Hs00980095_m1), and BIP/GRP78 (Hs00607129_gH) mRNA was normalized using GAPDH (Hs02758991_g1) as an invariant control. Subsequently, the relative quantification was obtained comparing the untreated vs. treatment samples by means of the calculation of $2^{-\Delta\Delta Ct}$.

Western Blot Analysis

Briefly, for western blot analysis, 30 μg of protein was loaded onto a 12% polyacrylamide gel MiniPROTEAN® TGX™ (BIO-RAD, Milan, Italy) followed by electrotransfer to nitrocellulose membrane TransBlot® Turbo™ (BIO-RAD, Milan, Italy) using TransBlot® SE Semi-Dry Transfer Cell (BIO-RAD, Milan, Italy). Subsequently, membrane was blocked in Odyssey Blocking Buffer (Licor, Milan, Italy) for 1 h at room temperature. After blocking, membrane was three times washed in phosphate-buffered saline (PBS) for 5 min and incubated with primary antibodies against HO-1 (1:1000) (anti-rabbit, cat. no. BML-HC3001-0025, Enzo Life Sciences, Milan, Italy), BiP (1:1000) (anti-rabbit, cat. no. 3177S, Cell Signaling Technology, Milan, Italy), iron-responsive element1 α (IRE1 α) (1:1000) (anti-rabbit, cat. no. 3294S, Cell Signaling Technology, Milan, Italy), and β -actin (1:1000) (anti-mouse, cat. no. 4967S, Cell Signaling Technology, Milan, Italy), overnight at 4 °C. Next day, membranes were three times washed in PBS for 5 min and incubated with infrared anti-mouse IRDye800CW (1:5000) and anti-rabbit IRDye700CW secondary antibodies (1:5000) in PBS/0.5% Tween-20 for 1 h at room temperature. All antibodies were diluted in Odyssey Blocking Buffer. The blots were visualized using Odyssey Infrared Imaging Scanner (Licor, Milan, Italy), and protein levels were quantified by densitometric analysis. Data were normalized to β -actin expression [33].

Immunofluorescence

Cells were grown directly on coverslips before immunofluorescence. After washing with PBS, cells were fixed in 4% paraformaldehyde (Sigma-Aldrich, Milan, Italy)

for 20 min at room temperature. Subsequently, cells were incubated with primary antibody against HO-1 (anti-rabbit, cat. no. BMLHC3001-0025, Enzo Life Sciences, Milan, Italy) at dilution 1:200, overnight at 4 °C. Next day, cells were washed three times in PBS for 5 min and incubated with secondary antibodies: TRITC (anti-mouse, cat. no. sc-3796, Santa Cruz Biotechnology) at dilution 1:200, and FITC (anti-rabbit, cat. no. sc-2012, Santa Cruz Biotechnology, Santa Cruz, CA, USA) at dilution 1:200 for 1 h at room temperature. The slides were mounted with medium containing DAPI (4',6-diamidino-2-phenylindole, Santa Cruz Biotechnology, Santa Cruz, CA, USA) to visualize nuclei. The fluorescent images were obtained using a Zeiss Axio Imager Z1 Microscope with Apotome 2 system (Zeiss, Milan, Italy). As a control, the specificity of immunostaining was verified by omitting incubation with the primary or secondary antibody. Immunoreactivity was evaluated taking into account the signal-to-noise ratio of immunofluorescence.

Mitogen-Activated Protein Kinase (MAPK) Phosphorylation Assessment by In-Cell Western

Cells were then fixed in 4% paraformaldehyde (PFA) by adding 20 μl of 12% PFA directly to the wells for 1 h at room temperature. The 96 wells were washed three times with PBS (50 μl /well), permeabilized with PBS/0.1% Triton X-100 (50 μl /well, three times, 2 min each), and blocked in LI-COR buffer (50 μl /well) for 2 h at room temperature (or alternatively overnight at 4 °C). The wells were then incubated with mouse anti-ERK1/2 or rabbit anti-phospho-ERK1/2 antibodies, mouse anti-JNK or rabbit anti-phospho-JNK antibodies, and mouse anti-p38 or rabbit anti-phospho-p38 antibodies (1:200 for optimal signal-to-noise ratio, Cell Signalling) in LI-COR blocking buffer for 2 h at room temperature (20 μl /well) and subsequently washed with PBS/0.1% Tween-20 (50 μl /well, three times). Infrared anti-mouse IRDye800CW and anti-rabbit IRDye700CW secondary antibodies (1:200) in PBS/0.5% Tween-20 were then added (20 μl /well). The plates were incubated for 1 h at room temperature, and the wells were washed with PBS/0.1% Tween-20 (three times) and incubated in PBS (50 μl /well). The plates were covered with black seals and imaged on an Odyssey infrared scanner using microplate settings with sensitivity of 5 in both the 700 and 800 nm wavelength channels. In separate wells, secondary antibodies alone were used to calculate background to be subtracted by the remaining wells. Data were acquired by using Odyssey software, exported and analyzed in Excel (Microsoft, Redmond, WA). Results were expressed as ratio between total ERK1/2 and phospho-ERK1/2, total JNK and phospho-JNK.

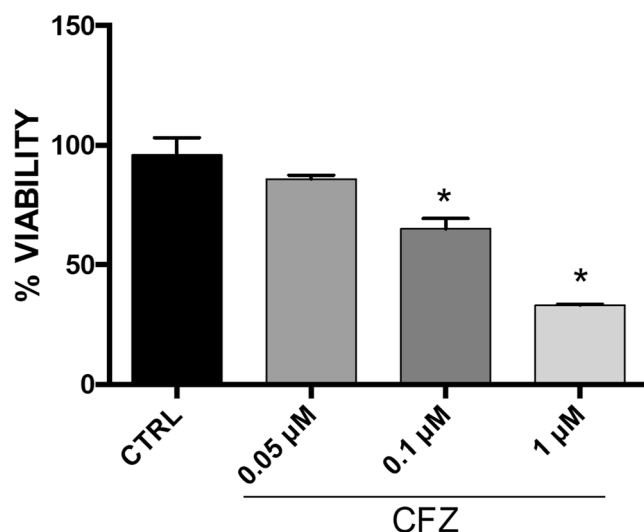
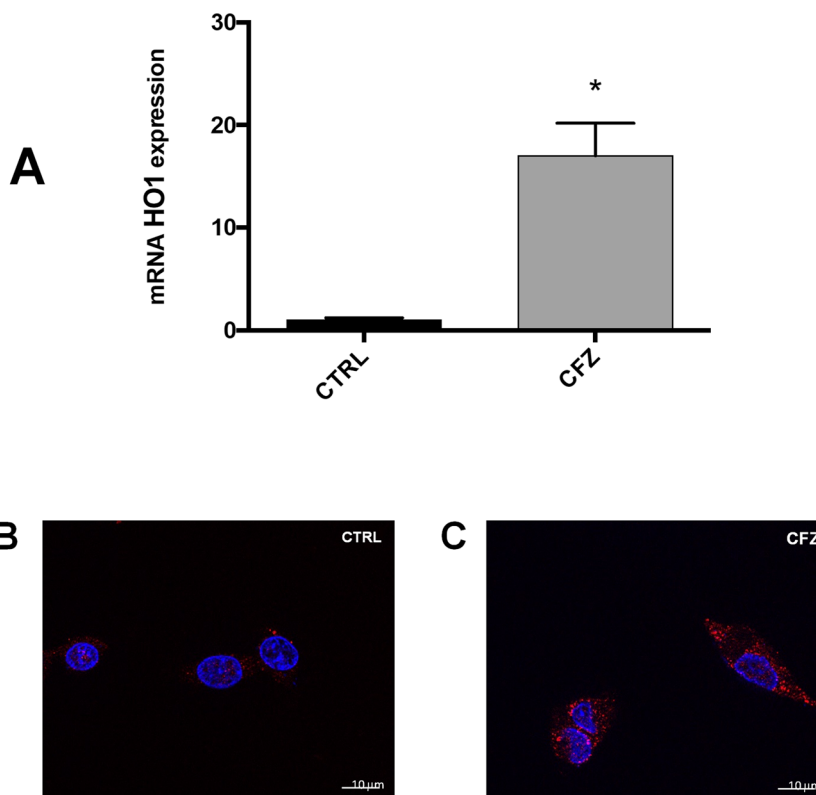


Fig. 1 Determination of cell viability of NB cell lines. ATPLite analysis for cell viability evaluation of NB cell lines untreated and treated by CFZ for 24 h at different concentration. The data are expressed as mean \pm SD (standard error) of five independent experiments. The significance of differences between means was analyzed by analysis of variance ($*p < 0.05$ respect to CTRL)

Statistical Analysis

The data are expressed as mean \pm SEM. Statistical analysis was carried out by ANOVA test: it is used to compare the means of more than two samples. The significance of

Fig. 2 Evaluation of HO-1 gene expression and HO activity on NB cell lines. **a** Evaluation of HO-1 gene expression in control cells and after treatment by CFZ (0.1 μ M). **b, c** Evaluation of HO-1 protein expression performed by incubation with anti-rabbit secondary antibody followed by monoclonal antibody conjugated with TRITC (red). The staining of the cells was performed using the nuclear dye DAPI (blue). Data are expressed as mean \pm SD of five independent experiments. The significance of differences between means was analyzed by analysis of variance ($*p < 0.05$ respect to CTRL)



differences between means was analyzed by analysis of variance. A p value of less than 0.05 ($*p < 0.05$) was accepted as statistically significant between experimental and control groups.

Results

Effect of CFZ on Cell Viability and Heme Oxygenase-1 Expression

CFZ treatment resulted in a significant and dose dependent reduction of cell viability (Fig. 1). In particular, we observed that after 24 h of CFZ treatment cell viability was significantly reduced by about 60 and 40% following 1 and 0.1 μ M CFZ, respectively. No significant effect was observed following with the dose of 0.05 μ M of CFZ (Fig. 1). Our results also showed that CFZ treatment resulted in a significant increase of HO-1 gene (Fig. 2a) and protein expression (Fig. 2b).

Role of Heme Oxygenase in CFZ-Induced Cytotoxicity

In order to investigate the effect of HO-1 in CFZ-mediated cytotoxicity, we treated cells with nor inducer (hemin) or inhibitor (SnMP) of HO-1 alone and in combination with 0.1 μ M CFZ. We showed that different

concentration of Hemin (1 and 10 μM) and SnMP were not toxic for cells (Fig. 3a). Interestingly, treatment with hemin (1 and 10 μM) abolished CFZ-mediated cytotoxicity whereas HO-1 inhibition (SnMP 10 μM) was not able to enhance CFZ-mediated cytotoxicity when compared to CFZ alone (Fig. 3b). We further tested the involvement of HO-1 under our experimental condition by specifically silencing HO-1 expression by mean of siRNA (siHMOX1). This set of experiments showed that siHMOX1 further enhanced CFZ-mediated cytotoxicity when compared to CFZ alone (Fig. 3b).

LS1/71 Sensitizes Cells to the Cytotoxic Effect of the CFZ

These set of experiments were aimed at evaluating the impact of selective HO-1 inhibition of CFZ toxicity. As a results of HO-1 non-competitive inhibition, LS1/71 significantly increased CFZ toxicity in neuroblastoma cells (Fig. 4a). In particular, 0.05 μM CFZ significantly reduced cell viability in the presence of LS1/71 when compared to CFZ or

untreated cells (Fig. 4b). Interestingly, LS1/71 resulted also in a significant decrease of HO-1 gene expression when compared to CFZ alone or untreated cells (Fig. 5a). Our results also showed that LS1/71 reduced CFZ-mediated HO activity increase (Fig. 5b).

LS1/71 Induced Apoptosis in NB Cells Treated with CFZ by ER Stress

To further evaluate the possible biochemical mechanism of LS1/71, we also investigated the possible involvement of endoplasmic reticulum stress (ER stress). We showed that CFZ treatment was able to increase ER stress as measured by PERK (Fig. 6b), IRE1 α (Fig. 6c), and GRP78 (Fig. 6d) protein expression. Furthermore, the combined treatment of CFZ with LS1/71, was able to further increase GRP/78 when compared to CFZ alone. Interestingly such treatment resulted also in a significant increase of the apoptotic gene BAX (Fig. 7a) while decreasing the antiapoptotic BCL2 gene expression (Fig. 7b). Consistently with these observation, we also observed a significant increase of CHOP (Fig. 7c) expression, an inducer of apoptosis mediated by ER stress.

Effect of LS1/71 and CFZ on Mitogen-Activated Protein Kinase

In order to assess the involvement of mitogen-activated protein kinases (MAPKs) on activation of apoptosis following treatment with CFZ-LS1/71, we measured phosphorylation of ERK, JNK, and p38 by in cell-western analysis. Surprisingly, the results showed an increased phosphorylation of ERK and JNK after exposure to CFZ (Fig. 8). Following treatment with the combination of CFZ and LS1/71, the phosphorylation of ERK and JNK was significantly reduced compared to CFZ alone or untreated cells. Finally, no significant change was observed in the phosphorylation of p38 (data not shown).

Discussion

PIs represent the first-line therapy for multiple myeloma patients and recent evidence suggest that they may be exploited as chemotherapeutic agents for solid tumors including NB [6]. In particular, previous studies evaluated the efficacy of PIs with traditional therapies such as doxorubicin [5, 34]. However, the clear biochemical molecular and molecular cut underlying the pharmacological mechanisms remain to be elucidated. To this regard, our previous data suggested that HO-1 may represent a possible molecular target of PIs toxicity as well as a key element in the mechanisms of chemoresistance [35].

In this study, we investigated the effect of non-competitive inhibition of HO-1 activity, by LS1/71 in

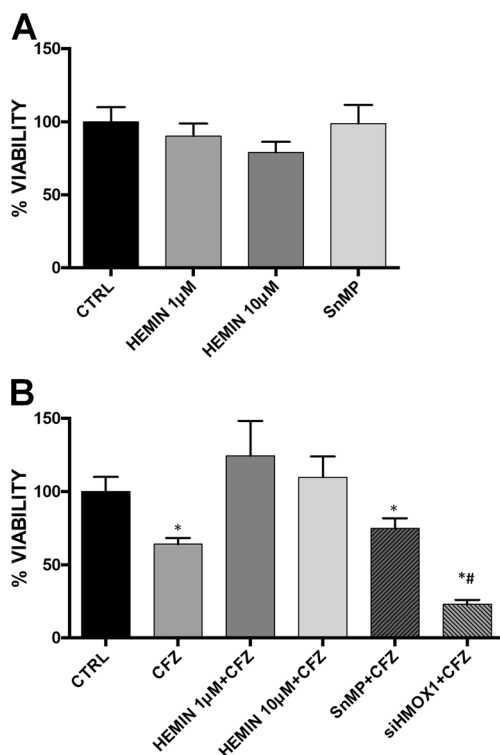


Fig. 3 Determination of cell viability of NB cell lines. **a** ATPLite analysis for cell viability evaluation of NB cell lines untreated (CTRL), treated by 1 and 10 μM Hemin and treated by 10 μM SnMP. **b** Analysis for cell viability evaluation of NB cell lines untreated, treated by CFZ (0.1 μM), and by combination of CFZ and 1 or 10 μM hemin (hemin+CFZ), of 10 μM SnMP (SnMP+CFZ) and by siHMOX1 (siHMOX1+CFZ). Data are expressed as mean \pm SD of five independent experiments. The significance of differences between means was analyzed by analysis of variance (* $p < 0.05$ respect to CTRL) (# $p < 0.05$ respect to CFZ)

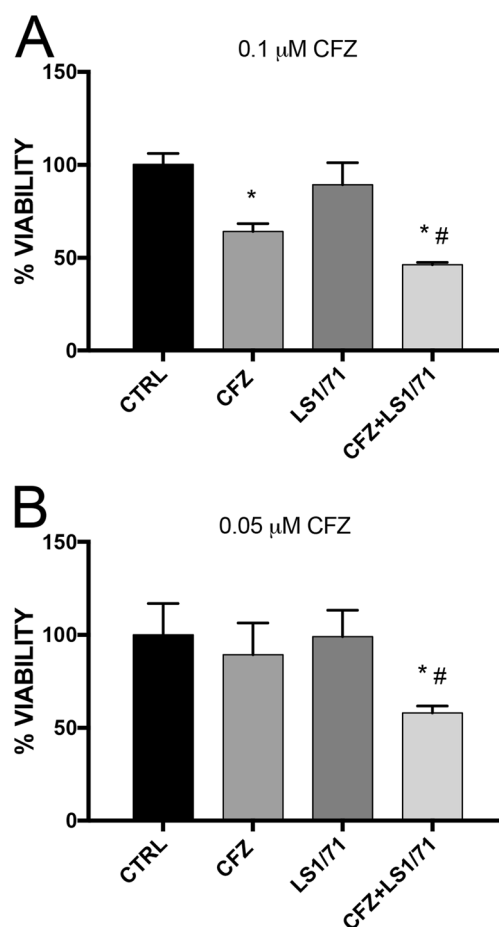


Fig. 4 Determination of cell viability of NB cell lines. **a** Analysis for cell viability evaluation of NB cell lines untreated, treated by CFZ (0.1 μM), treated by 10 μM LS1/71 and by combination of CFZ and LS1/71 (CFZ+LS1/71). **b** Analysis for cell viability evaluation of NB cell lines untreated, treated by CFZ (0.05 μM), treated by 10 μM LS1/71 and by

combination of CFZ and LS1/71 (CFZ+LS1/71). Data are expressed as mean \pm SD of five independent experiments. The significance of differences between means was analyzed by analysis of variance. (* $p < 0.05$ respect to CTRL) (# $p < 0.05$ respect to CFZ)

NB cells and how such pharmacological treatment impact on CFZ mediated cytotoxicity. Inhibition of HO activity by metalloporphyrins (i.e., SnMP or ZnPPiX) has several drawbacks since they do not discriminate between the two isoforms and exhibit non specific activity on other heme-containing enzymes such as nitric oxide synthase (NOS), and cytochromes, and may be also a potent inducer of HO-1. Therefore, in order to develop more specific HO-1 inhibitors, devoid of the typical side-effects of Mps, in a recent study Salerno et al. designed and synthesized a novel series of imidazole-based HO-1 inhibitors structurally different from MPs. (1-[4-(4-iodophenoxy)butyl]-1*H*-imidazole), named LS1/71, showing the highest selective inhibitory activity against HO-1 among this series. LS1/71 was used in combination with imatinib in leukemia cells downregulating HO-1 expression and activity, abolishing pharmacological resistance [30, 36].

Our results showed that CFZ increased both HO-1 protein and gene expression which was dependent on

ER stress pathway activation. These results are consistent with our previous work showing that BTZ was also able to induce HO-1 in multiple myeloma via the activation of the UPR response triggered by ER stress. Furthermore, we also showed that such complex biochemical cascade of events lead to nuclear translocation of HO-1, thus conferring resistance to BTZ and inducing genetic instability in MM cells [35]. The involvement of HO-1 in CFZ mediated cytotoxicity is further substantiated by the protective effect of pharmacological induction of HO-1 (i.e. hemin) mitigating CFZ cytotoxicity. Consistently with these results, HO-1 gene silencing by a specific siRNA was able to increase the cytotoxic effect induced by CFZ in NB while inhibition of HO activity by SnMP, a competitive and non-specific inhibitor of HO activity, showed no significant change compared to treatment with only CFZ.

Therefore, in the present study we tested the effect of a new non-competitive inhibitor of HO-1 as a possible adjuvant therapy to overcome drug resistance and

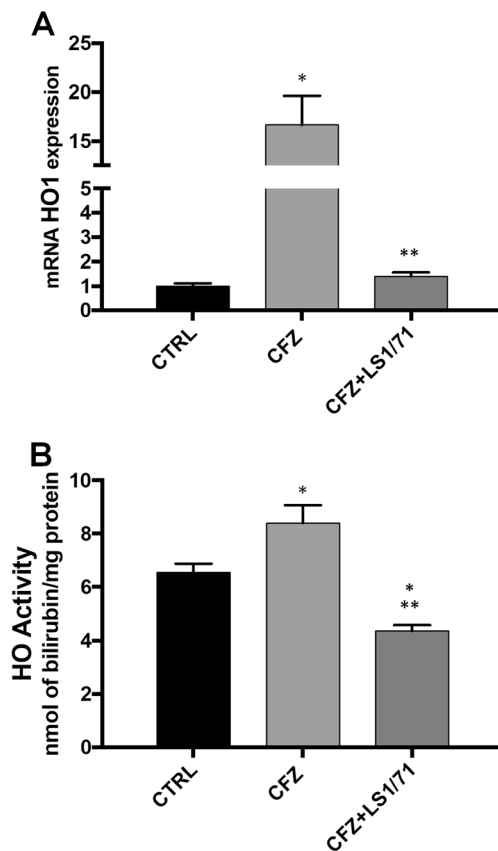
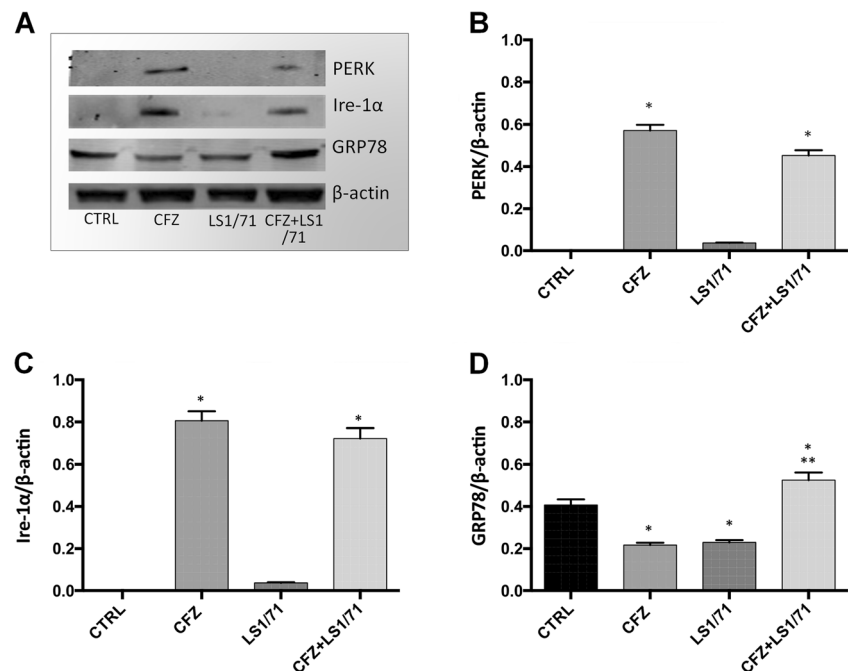


Fig. 5 Evaluation of HO activity and HO-1 gene expression on NB cell lines. **a** Evaluation of HO-Activity in control cells (CTRL), after treatment by CFZ (0.05 μ M) and by combination of CFZ and LS1/71 (CFZ+LS1/71). **b** Evaluation of HO-1 gene expression in control cells (CTRL), after treatment by CFZ (0.05 μ M) and by combination of CFZ and LS1/71 (CFZ+LS1/71)

Fig. 6 a Western Blot analysis. Densitometric analysis of chaperon levels of PERK (**b**), IRE1 α (**c**), and GRP78 (**d**) protein expression in neuroblastoma cell lines untreated, treated by CFZ (0.05 μ M), treated by 10 μ M LS1/71 and by combination of CFZ and LS1/71 (CFZ + LS1/71). The data are expressed as mean \pm SD of five independent experiments. The significance of differences between means was analyzed by analysis of variance. (* p < 0.05 respect to CTRL) (** p < 0.05 respect to CFZ)



potentiating the efficacy of CFZ. This set of experiments showed that LS1/71 was able to decrease cell viability following CFZ treatment. Interestingly, our results showed that LS1/71 sensitized cells to lower concentrations of CFZ (i.e., 0.05 μ M). Finally, our data indicated that when cells are treated with CFZ or LS1/71, CHOP apoptotic pathway is activated together with the pro-apoptotic BAX gene while the BFAR, antiapoptotic gene, is significantly reduced. These data suggest that treatment with CFZ produces ER stress in NB without activating CHOP-mediated apoptosis, whereas CFZ and LS1/71 co-treatment determined apoptosis activation and induction of CHOP expression.

Ultimately, CFZ treatment resulted also in the activation of ERK and JNK signal transduction pathways whereas LS1/71 decreased phosphorylation of ERK and JNK and thus leading to a reduction of cell proliferation and increased apoptosis following proteasome inhibition.

In conclusion, our study showed that treatment with the non-competitive inhibitor of HO-1, LS1/71 demonstrating different biochemical and pharmacological profile increased CFZ mediated cytotoxicity by triggering apoptosis following ER stress activation. Taken all together, these results also suggest that PIs may represent a possible pharmacological treatment for solid tumors and that HO-1 inhibition may represent a possible strategy to overcome chemoresistance and increase the efficacy of chemotherapeutic regimens.

Fig. 7 Evaluation of Gene BAX (a), BFAR (b), and CHOP (c) gene expression in neuroblastoma cell lines untreated, treated by CFZ (0.05 μ M), treated by 10 μ M LS1/71 and by combination of CFZ and LS1/71 (CFZ+LS1/71). The data are expressed as mean \pm SD of five independent experiments. The significance of differences between means was analyzed by analysis of variance. (* p < 0.05 respect to CTRL) (# p < 0.05 respect CFZ)

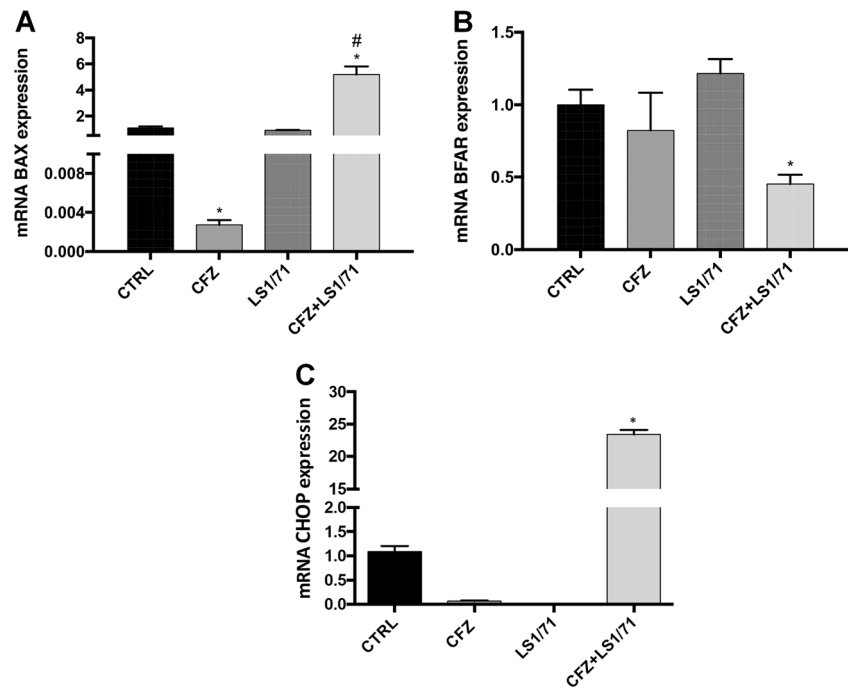
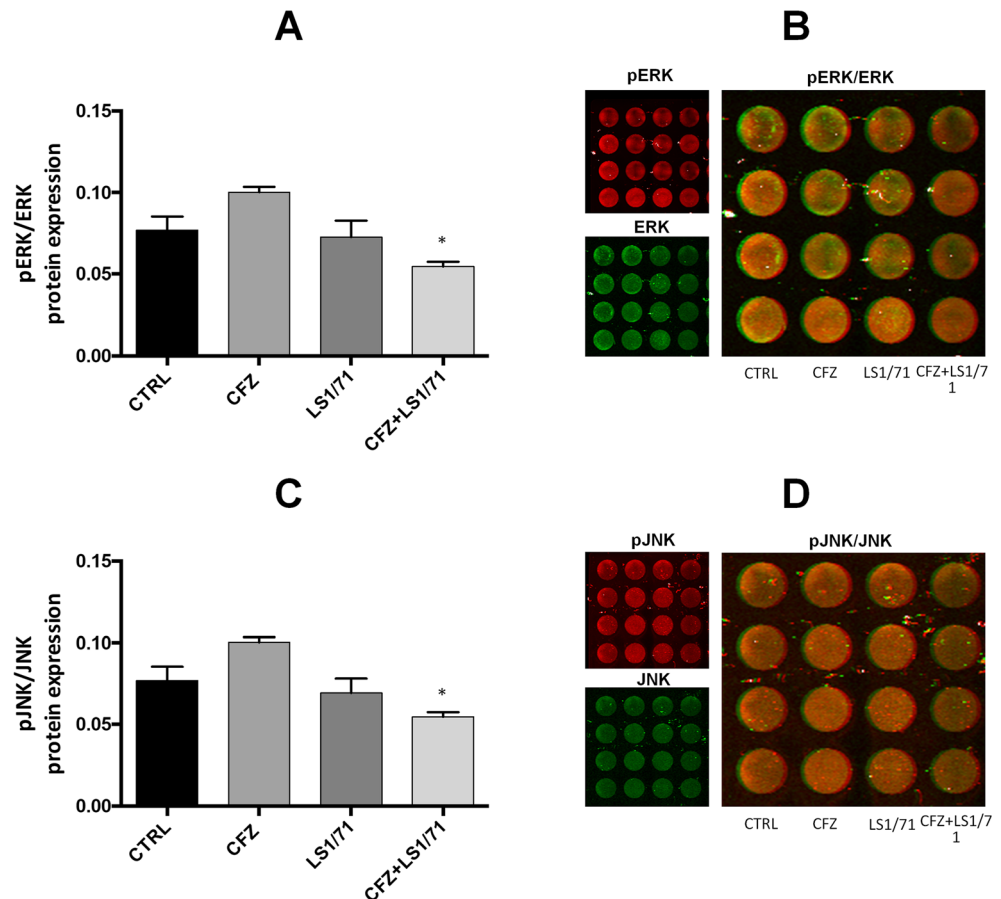


Fig. 8 Evaluation of ERK (a, b) and JNK (b, c, d) phosphorylation by in cell-western analysis. Measurement of ratio between phospho ERK and total ERK protein expression, and between phospho JNK and total JNK protein expression in neuroblastoma cell lines untreated, treated by CFZ (0.05 μ M), treated by 10 μ M LS1/71 and by combination of CFZ and LS1/71 (CFZ + LS1/71). The significance of differences between means was analyzed by analysis of variance (* p < 0.05 respect to CTRL)



Acknowledgments This work was financially supported by Fir 2017 from the University of Catania (PI: Loredana Salerno).

References

- Hoehner JC, Gestblom C, Hedborg F, Sandstedt B, Olsen L, Pahlman S (1996) A developmental model of neuroblastoma: differentiating stroma-poor tumors' progress along an extra-adrenal chromaffin lineage. *Lab Invest* 75(5):659–675
- Lev N, Melamed E, Offen D (2006) Proteasomal inhibition hypersensitizes differentiated neuroblastoma cells to oxidative damage. *Neurosci Lett* 399(1–2):27–32. <https://doi.org/10.1016/j.neulet.2005.09.086>
- Johnson DE (2015) The ubiquitin-proteasome system: opportunities for therapeutic intervention in solid tumors. *Endocr Relat Cancer* 22(1):T1–T17. <https://doi.org/10.1530/ERC-14-0005>
- Furfaro AL, Piras S, Domenicotti C, Fenoglio D, De Luigi A, Salmons M, Moretta L, Marinari UM et al (2016) Role of Nrf2, HO-1 and GSH in neuroblastoma cell resistance to bortezomib. *PLoS One* 11(3):e0152465. <https://doi.org/10.1371/journal.pone.0152465>
- Guan S, Zhao Y, Lu J, Yu Y, Sun W, Mao X, Chen Z, Xu X et al (2016) Second-generation proteasome inhibitor carfilzomib sensitizes neuroblastoma cells to doxorubicin-induced apoptosis. *Oncotarget* 7(46):75914–75925. <https://doi.org/10.18632/oncotarget.12427>
- Mody R, Zhao L, Yanik GA, Opirari V (2017) Phase I study of bortezomib in combination with irinotecan in patients with relapsed/refractory high-risk neuroblastoma. *Pediatr Blood Cancer* 64(11). <https://doi.org/10.1002/pbc.26563>
- Furfaro AL, Piras S, Passalacqua M, Domenicotti C, Parodi A, Fenoglio D, Pronzato MA, Marinari UM et al (2014) HO-1 up-regulation: A key point in high-risk neuroblastoma resistance to bortezomib. *Biochim Biophys Acta* 1842(4):613–622. <https://doi.org/10.1016/j.bbadis.2013.12.008>
- Tibullo D, Giallongo C, Puglisi F, Tomassoni D, Camiolo G, Cristaldi M, Brundo MV, Anfosso CD et al (2017) Effect of lipoic acid on the biochemical mechanisms of resistance to bortezomib in SH-SY5Y neuroblastoma cells. *Mol Neurobiol* 55:3344–3350. <https://doi.org/10.1007/s12035-017-0575-6>
- Valentiner U, Haane C, Nehmann N, Schumacher U (2009) Effects of bortezomib on human neuroblastoma cells in vitro and in a metastatic xenograft model. *Anticancer Res* 29(4):1219–1225
- Ohta T, Iijima K, Miyamoto M, Nakahara I, Tanaka H, Ohtsuji M, Suzuki T, Kobayashi A et al (2008) Loss of Keap1 function activates Nrf2 and provides advantages for lung cancer cell growth. *Cancer Res* 68(5):1303–1309. <https://doi.org/10.1158/0008-5472.CAN-07-5003>
- Jiang T, Chen N, Zhao F, Wang XJ, Kong B, Zheng W, Zhang DD (2010) High levels of Nrf2 determine chemoresistance in type II endometrial cancer. *Cancer Res* 70(13):5486–5496. <https://doi.org/10.1158/0008-5472.CAN-10-0713>
- Shibata T, Kokubu A, Gotoh M, Ojima H, Ohta T, Yamamoto M, Hirohashi S (2008) Genetic alteration of Keap1 confers constitutive Nrf2 activation and resistance to chemotherapy in gallbladder cancer. *Gastroenterology* 135(4):1358–1368. <https://doi.org/10.1053/j.gastro.2008.06.082> 1368 e1351–1354
- Tibullo D, Barbagallo I, Giallongo C, La Cava P, Parrinello N, Vanella L, Stagno F, Palumbo GA et al (2013) Nuclear translocation of heme oxygenase-1 confers resistance to imatinib in chronic myeloid leukemia cells. *Curr Pharm Des* 19(15):2765–2770
- Salerno L, Romeo G, Modica MN, Amata E, Sorrenti V, Barbagallo I, Pittala V (2017) Heme oxygenase-1: A new druggable target in the management of chronic and acute myeloid leukemia. *Eur J Med Chem* 142:163–178. <https://doi.org/10.1016/j.ejmech.2017.07.031>
- Jozkowicz A, Was H, Dulak J (2007) Heme oxygenase-1 in tumors: Is it a false friend? *Antioxid Redox Signal* 9(12):2099–2117. <https://doi.org/10.1089/ars.2007.1659>
- Barbagallo I, Galvano F, Frigiola A, Cappello F, Riccioni G, Murabito P, D'Orazio N, Torella M et al (2013) Potential therapeutic effects of natural heme oxygenase-1 inducers in cardiovascular diseases. *Antioxid Redox Signal* 18(5):507–521. <https://doi.org/10.1089/ars.2011.4360>
- Barbagallo I, Nicolosi A, Calabrese G, David S, Cimino S, Madonia M, Cappello F (2014) The role of the heme oxygenase system in the metabolic syndrome. *Curr Pharm Des* 20(31):4970–4974
- Li Volti G, Tibullo D, Vanella L, Giallongo C, Di Raimondo F, Forte S, Di Rosa M, Signorelli SS et al (2017) The Heme oxygenase system in hematological malignancies. *Antioxid Redox Signal* 27(6):363–377. <https://doi.org/10.1089/ars.2016.6735>
- Goodman AI, Choudhury M, da Silva JL, Schwartzman ML, Abraham NG (1997) Overexpression of the heme oxygenase gene in renal cell carcinoma. *Proc Soc Exp Biol Med Soc* 214(1):54–61
- Maines MD, Abrahamson PA (1996) Expression of heme oxygenase-1 (HSP32) in human prostate: Normal, hyperplastic, and tumor tissue distribution. *Urology* 47(5):727–733
- Berberat PO, Dambrauskas Z, Gulbinas A, Giese T, Giese N, Kunzli B, Autschbach F, Meuer S et al (2005) Inhibition of heme oxygenase-1 increases responsiveness of pancreatic cancer cells to anticancer treatment. *Clin Cancer Res* 11(10):3790–3798. <https://doi.org/10.1158/1078-0432.CCR-04-2159>
- Furfaro AL, Macay JR, Marengo B, Nitti M, Parodi A, Fenoglio D, Marinari UM, Pronzato MA et al (2012) Resistance of neuroblastoma GI-ME-N cell line to glutathione depletion involves Nrf2 and heme oxygenase-1. *Free Radic Biol Med* 52(2):488–496. <https://doi.org/10.1016/j.freeradbiomed.2011.11.007>
- Barbagallo I, Parenti R, Zappala A, Vanella L, Tibullo D, Pepe F, Onni T, Li Volti G (2015) Combined inhibition of Hsp90 and heme oxygenase-1 induces apoptosis and endoplasmic reticulum stress in melanoma. *Acta Histochem* 117(8):705–711. <https://doi.org/10.1016/j.acthis.2015.09.005>
- Vanella L, Barbagallo I, Tibullo D, Forte S, Zappala A, Li Volti G (2016) The non-canonical functions of the heme oxygenases. *Oncotarget* 7(42):69075–69086. <https://doi.org/10.18632/oncotarget.11923>
- Morioka I, Wong RJ, Abate A, Vreman HJ, Contag CH, Stevenson DK (2006) Systemic effects of orally-administered zinc and tin (IV) metalloporphyrins on heme oxygenase expression in mice. *Pediatr Res* 59(5):667–672. <https://doi.org/10.1203/01.pdr.0000215088.71481.a6>
- Pittala V, Salerno L, Romeo G, Modica MN, Siracusa MA (2013) A focus on heme oxygenase-1 (HO-1) inhibitors. *Curr Med Chem* 20(30):3711–3732
- Sorrenti V, Guccione S, Di Giacomo C, Modica MN, Pittala V, Acquaviva R, Basile L, Pappalardo M et al (2012) Evaluation of imidazole-based compounds as heme oxygenase-1 inhibitors. *Chem Biol Drug Des* 80(6):876–886. <https://doi.org/10.1111/cbdd.12015>
- Salerno L, Pittala V, Romeo G, Modica MN, Marrazzo A, Siracusa MA, Sorrenti V, Di Giacomo C et al (2015) Novel imidazole derivatives as heme oxygenase-1 (HO-1) and heme oxygenase-2 (HO-2) inhibitors and their cytotoxic activity in human-derived cancer cell lines. *Eur J Med Chem* 96:162–172. <https://doi.org/10.1016/j.ejmech.2015.04.003>
- Amata E, Marrazzo A, Dichiaro M, Modica MN, Salerno L, Prezzavento O, Nastasi G, Rescifina A et al (2017) Heme oxygenase database (HemeOxDB) and QSAR analysis of isoform 1

- inhibitors. *ChemMedChem* 12(22):1873–1881. <https://doi.org/10.1002/cmdc.201700321>
30. Salerno L, Pittala V, Romeo G, Modica MN, Siracusa MA, Di Giacomo C, Acquaviva R, Barbagallo I et al (2013) Evaluation of novel aryloxyalkyl derivatives of imidazole and 1,2,4-triazole as heme oxygenase-1 (HO-1) inhibitors and their antitumor properties. *Bioorg Med Chem* 21(17):5145–5153. <https://doi.org/10.1016/j.bmc.2013.06.040>
 31. Pittala V, Siracusa MA, Modica MN, Salerno L, Pedretti A, Vistoli G, Cagnotto A, Mennini T et al (2011) Synthesis and molecular modeling of 1H-pyrrolopyrimidine-2,4-dione derivatives as ligands for the alpha1-adrenoceptors. *Bioorg Med Chem* 19(17):5260–5276. <https://doi.org/10.1016/j.bmc.2011.06.043>
 32. Ryter SW, Alam J, Choi AM (2006) Heme oxygenase-1/carbon monoxide: From basic science to therapeutic applications. *Physiol Rev* 86(2):583–650. <https://doi.org/10.1152/physrev.00011.2005>
 33. Tibullo D, Barbagallo I, Giallongo C, La Cava P, Branca A, Conticello C, Stagno F, Chiarenza A et al (2012) Effects of second-generation tyrosine kinase inhibitors towards osteogenic differentiation of human mesenchymal cells of healthy donors. *Hematol Oncol* 30(1):27–33. <https://doi.org/10.1002/hon.988>
 34. Li H, Chen Z, Hu T, Wang L, Yu Y, Zhao Y, Sun W, Guan S et al (2016) Novel proteasome inhibitor ixazomib sensitizes neuroblastoma cells to doxorubicin treatment. *Sci Rep* 6:34397. <https://doi.org/10.1038/srep34397>
 35. Tibullo D, Barbagallo I, Giallongo C, Vanella L, Conticello C, Romano A, Saccone S, Godos J et al (2016) Heme oxygenase-1 nuclear translocation regulates bortezomib-induced cytotoxicity and mediates genomic instability in myeloma cells. *Oncotarget* 7(20):28868–28880. <https://doi.org/10.18632/oncotarget.7563>
 36. Salerno L, Amata E, Romeo G, Marrazzo A, Prezzavento O, Floresta G, Sorrenti V, Barbagallo I et al (2018) Potholing of the hydrophobic heme oxygenase-1 western region for the search of potent and selective imidazole-based inhibitors. *Eur J Med Chem* 148:54–62. <https://doi.org/10.1016/j.ejmech.2018.02.007>